MDPI

Article

A 278-Year Summer Minimum Temperature Reconstruction Based on Tree-Ring Data in the Upper Reaches of Dadu River

Jinjian Li [1,2], **Liya Jin** [1,2,*] **and Zeyu Zheng** [1]

1   MOE Key Laboratory of Western China's Environmental System, College of Earth and Environmental Sciences, Lanzhou University, Lanzhou 730000, China; ljj@cuit.edu.cn (J.L.); zhengzy17@lzu.edu.cn (Z.Z.)
2   Plateau Atmosphere and Environment Key Laboratory of Sichuan Province, School of Atmospheric Sciences, Chengdu University of Information Technology, Chengdu 610225, China
*   Correspondence: jinly@lzu.edu.cn

Abstract: In the context of global warming, climate change in river headwater regions and its drivers have attracted increasing attention. In this study, tree-ring width (TRW) chronology was constructed using tree-ring samples of fir (*Abies faxoniana*) in Dadu River Basin in the central part of the western Sichuan Plateau, China. Correlation analysis with climatic factors implies that the radial growth of trees in the region is mainly limited by temperature and has the highest correlation with the mean minimum temperature in summer (June and July) ($R = 0.602$, $p < 0.001$). On this basis, the TRW chronology was adopted to reconstruct variations in the mean minimum temperatures in summer from 1733 to 2010 in the upper reaches of Dadu River. The reconstruction equation was stable and reliable and offered a variance explanation rate of 36.2% in the observed period (1962~2010). In the past 278 years, the region experienced nine warm periods and ten cold periods. The warmest and coldest years occurred in 2010 and 1798, respectively, with values of 13.6 °C and 11.0 °C. The reconstruction was highly spatiotemporally representative and verified by temperatures reconstructed using other tree-ring data in surrounding areas. A significant warming trend was found in the last few decades. Moreover, the multi-taper method (MTM) analysis indicated significant periodic changes in quasi-2-year and 21–35-year periods, for which the El Niño Southern Oscillation (ENSO) and the Pacific decadal oscillation (PDO) could be the key controlling factors.

Keywords: tree ring; temperature reconstruction; up catch of river; climate change; China

1. Introduction

The short-term instrument measurements and sparse distribution of meteorological stations are the main factors that limit our understanding of regional climate change, particularly in alpine and plateau regions [1,2]. Additionally, to reveal the characteristics, causes, and trends of climate change at various temporal and spatial scales and forecast future climate change and its impacts, long-term climate records are needed [3,4]. Existing research and analysis of historical climate change generally rely on climate proxy data, particularly high-resolution climate proxy data. These data not only provide important basic information for verifying climate modes but also play a crucial role in understanding the characteristics and causes of climate and environmental changes, performing climatic predictions, and analyzing the relationship between human activities and climate change [5–7]. Numerous scholars have used climate proxy data such as ice cores, lacustrine sedimentary records, and historical literature to reconstruct climate change over the past several centuries and millennia [8–10]. Among diverse climate proxy data, tree-ring data are highly regarded due to their accurate dating and high time resolution. By using tree-ring data, multiple climate series were reconstructed, which revealed the trends and characteristics of historical climate change [11–14].

Recent research has shown that the Qinghai–Tibet Plateau (QTP) is the driver of climate change in China and the whole of East Asia [15,16]; as such, this area's climate-change

characteristics have attracted increasing attention. Located between the main part of QTP and the Sichuan Basin, the Western Sichuan Plateau (WSP), which is scarcely populated and covered by rich vegetation, is a transition zone from the alpine climate zone of the QTP to the subtropical climate prevailing in the Sichuan Basin [17,18]. Climate characteristics are of important scientific significance for determining climate change in the QTP, the nearby Sichuan Basin, and even the entirety of southwestern China. Since the 1990s, many tree-ring researchers have sampled tree rings in the WSP to reconstruct the climate changes at numerous locations in the plateau using the tree-ring width (TRW), maximum density, isotopes, etc. These researchers have made great efforts to reveal the historical climate changes over the past 100~500 years on the WSP [18–23]. Rivers are densely distributed over the WSP and breed important tributaries of the Yangtze River, including the Minjiang River, Dadu River, and Yalong River. However, existing tree-ring-based climatological research in the WSP mainly focuses on alpine timberline with old trees and mainly represents plateau climates, while attention to climate change in river regions remains to be improved [3]. Against this background, *Abies faxoniana* samples were collected by setting sampling points on slopes along banks of the main tributaries upstream of Dadu River in the central part of the WSP to construct the TRW's chronology. Based on an analysis of the relationship between the TRW and climatic factors, temperature variations in the last several hundred in the upper reaches of Dadu River were reconstructed, thus revealing temperature variations and enabling us to explore the possible drivers. This research expands our understanding of long-term climate change in river headwater regions and provides a scientific basis for ecological conservation in these regions.

2. Materials and Methods

2.1. Study Area and Tree-Ring Data

The tree-ring samples used in this research were collected from the Lover Sea scenic area in Maori Township, Aba Tibetan, and Qiang Autonomous Prefecture, Sichuan Province, China (101°42′ E, 31°31′ N, Figure 1). *Abies faxoniana* tree rings were collected at sampling points established on the slope of main tributaries upstream of Dadu River at an altitude of 3000 m. This region is within the range of the QTP climate zone. Under joint action of the jet stream in the Southern Branch of the westerlies, southeast monsoon, and southwest monsoon, a mountain climate affording a cold winter, cool summer, and moderate rainfall is formed in the region [17]. The annual mean temperature (1961~2010) is 10.6 °C, and the monthly mean temperature changes during the year are single-peaked, with the lowest temperature (0.9 °C) in January and the highest temperature (18.5 °C) in July. The annual mean precipitation (1961~2010) is 634.5 mm, and the monthly precipitation distribution shows a bimodal pattern, with peaks, respectively, in June and September. Tree cores were collected within several square kilometers (not exceeding 0.2 square kilometers) in the sampling points where the difference in elevation did not exceed 100 m. The forest depression of the sampling site was up to about 0.4. The trees were mostly healthy living trees, and the understory vegetation was rich, with common plants, such as rhododendron and lonicera, a denser grass cover layer, and scattered mosses of 10~30 mm. An increment borer was used to collect two tree cores (three from some trees) at breast height. A total of 59 cores were collected from 24 old trees.

All core samples were pre-processed following the basic international procedures for tree-ring analysis [24,25]. A Lintab system with a precision of 0.01 mm was used to measure the TRW, and the COFECHA software [26] was adopted for cross-dating. Afterward, the ARSTAN program [27] was used for detrending to eliminate non-climatic information contained in the original TRW and retain as much climatic information as possible. By repeatedly fitting the growth trend using different methods, the spline function with a step of 50 years was found to perform best in fitting the growth trend. Finally, we obtained three tree-ring chronologies: standard (STD), residual (RES), and autoregressive standard (ARS) chronologies [27]. Several core samples with large differences from the main series were eliminated in the process of constructing the chronologies. STD chronology was mainly

adopted for the analysis. The total length of the chronology was 336 years (1675~2010), and the average sensitivity was 0.158. In the common period of 1900~2000, the intra-tree and inter-tree correlation coefficients were, respectively, 0.604 and 0.208, and the expressed population signal (EPS), signal-to-noise ratio (SNR), and variance explained by the first principal component were, respectively, 0.943, 16.518, and 29.7%. These statistical characteristics of the chronologies indicate that the chronology has the potential to reflect past climate change. EPS > 0.85 was used to determine the reliable interval of the chronology [21,28]. After reaching 21 tree rings, the EPS exceeded 0.85, so the reliable period was deemed to be 1733~2010 (Table 1 and Figure 2).
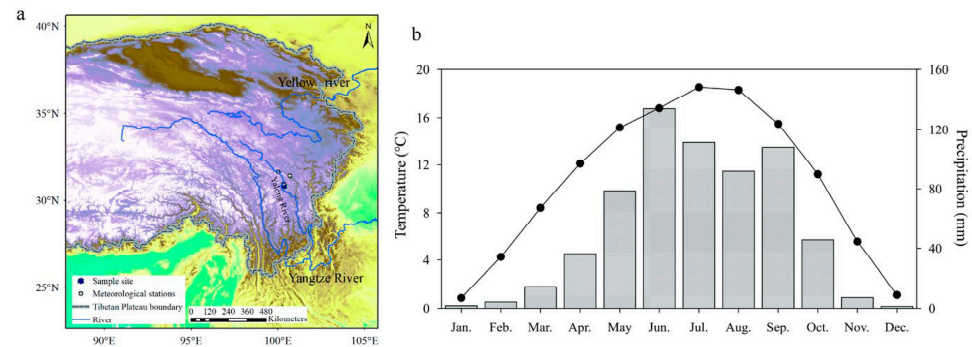

Figure 1. Locations of the sampling site, meteorological stations, (**a**) and monthly mean temperatures and total precipitation for the study area, which were calculated from 5 meteorological stations (Danba, Luhuo, Jinchuan, Xiaojin, and Daofu) during the period of 1962~2010 (**b**).

Table 1. Statistical characteristics of the chronology.

Statistical Characteristic	Values
Period	1675–2010
Common period	1900–2000
First-order autocorrelation (AC1)	0.773
Signal-to-noise ratio (SNR)	16.518
Mean sensitivity (MS)	0.158
Mean correlations within trees	0.604
Mean correlations between trees	0.208
Expressed population signal (EPS)	0.943
Period with EPS > 0.85 (minimum number of trees)	1733 (21)
Variance of first eigenvector (PC1)	29.7%

2.2. Meteorological Data

Meteorological data used in this study included monthly mean temperature, maximum temperature, minimum temperature, and precipitation from 1961 to 2010 recorded at five stations: Danba County (101°88′ E, 30°88′ N, at an altitude of 1950 m), Luhuo County (100°67′ E, 31°40′ N, at an altitude of 3250 m), Daofu County (101°12′ E, 30°98′ N, at an altitude of 2957 m), Jinchuan County (102°07′ E, 31°53′ N, at an altitude of 2169 m), and Xiaojin County (102°35′ E, 31° N, at an altitude of 2369 m). The mean values of climatic factors at the five stations were used to characterize the climatic characteristics of the study area. Sea surface temperatures were taken from the Extended Reconstructed Sea Surface Temperature V5 (ERSST V5) dataset with a spatial resolution of $2° \times 2°$ provided by the National Oceanic and Atmospheric Administration (NOAA).
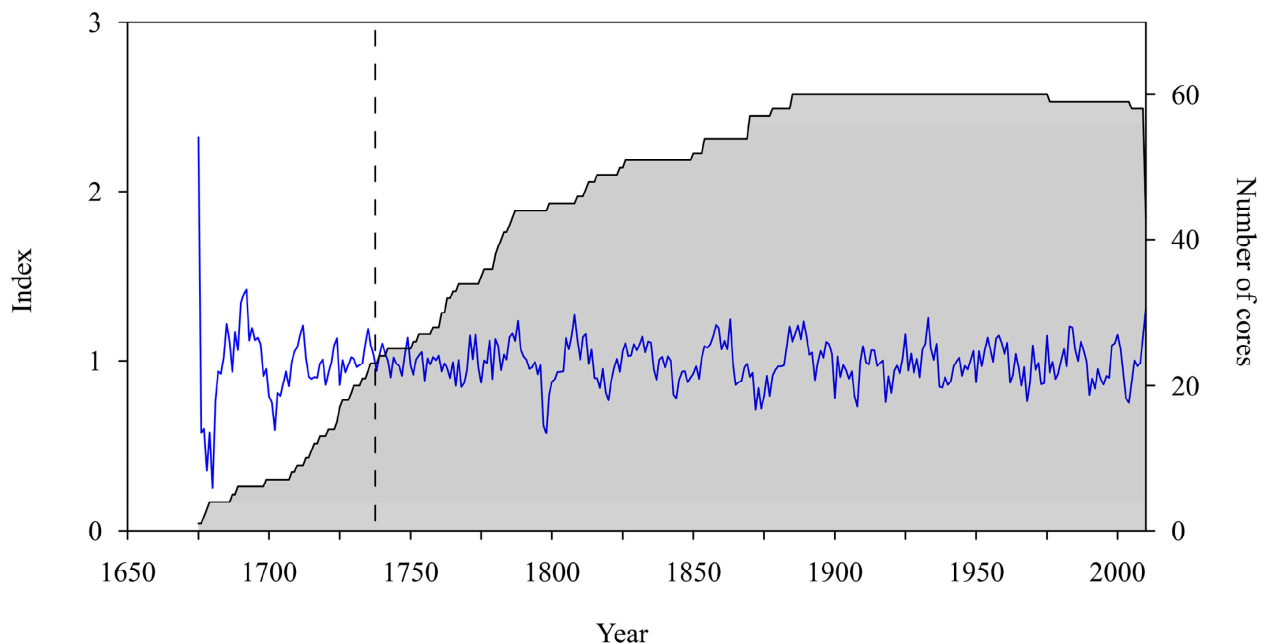
Figure 2. The tree ring width and number of tree rings. The red arrow indicates that the first year of EPS > 0.85.

2.3. Methods

Pearson's correlation analysis was used to identify the key climatic factors in this study. The method of leave-one-out cross-validation (LOOCV) was used to assess the stability and reliability of the reconstruction equation. The main statistic parameters were the correlation coefficient (R), variance explanation (R2), sign tests, sign tests of first-order difference, F value, mean product (t), and reduced error (RE) [24]. The standard deviation (SD) could reflect the degree of the dispersion of a data set; it was used to identify extreme climate events [18,21,29]. Here, a mean threshold of ± 1.5 times the standard deviation (SD) was used to judge years with extremely high and low temperatures. A year with a reconstructed temperature higher than the mean + 1.5SD was regarded as an extremely warm year; if the reconstructed temperature was lower than the mean -1.5SD, the year was considered to be an extremely cold year. To determine the decadal variations in cold and warm periods, time periods lower and higher than the mean temperature for more than nine successive years were defined as cold and warm periods, respectively, based on low-pass filtering of the reconstructed series for 11 years. The multi-taper method (MTM), which is a low-variance high-resolution spectral analysis method especially suitable for diagnostic analysis of quasi-periodic signals with short sequences and high noise background [30,31], was used to identify the cycle of reconstruction.

3. Results

3.1. Climate-Growth Response Analysis

Figure 3 illustrates correlations of the tree-ring index with regional climatic factors (including the mean temperature, maximum temperature, minimum temperature, and precipitation). Results showed that for correlations with precipitation, the radial growth of trees was significantly negatively correlated in the previous December (R = -0.346, $p < 0.05$) and significantly positively correlated with the current July (R = 0.321, $p < 0.05$). For correlations with the temperature, the radial growth of trees was significantly positively correlated with the mean and minimum temperatures in June and July of the current year (R = 0.528, 0.284, 0.503, and 0.489, respectively; $p < 0.05$) and the maximum temperatures in February and June of the current year (R = 0.283 and 0.5, respectively; $p < 0.05$). Therein, radial growth was the most significantly correlated with mean temperature in June, with a correlation coefficient of 0.528 ($p < 0.01$). Correlation analysis was also performed for climatic factors under different month

combinations. The results indicated that the mean minimum temperatures in June and July were most significantly correlated with the tree-ring index, with the correlation coefficient reaching 0.601 ($p < 0.01$). Meanwhile, the 31-year moving correlations also showed that the tree-ring index had a stable relationship with the climatic factors (Figure 4).
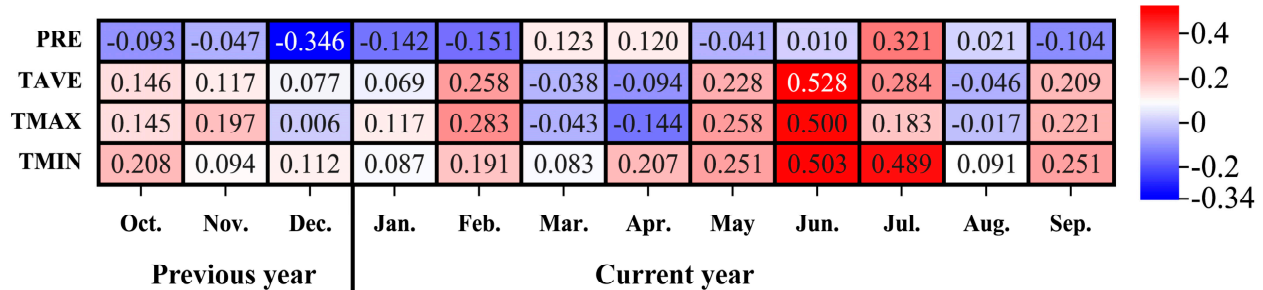

	Oct.	Nov.	Dec.	Jan.	Feb.	Mar.	Apr.	May	Jun.	Jul.	Aug.	Sep.
PRE	-0.093	-0.047	-0.346	-0.142	-0.151	0.123	0.120	-0.041	0.010	0.321	0.021	-0.104
TAVE	0.146	0.117	0.077	0.069	0.258	-0.038	-0.094	0.228	0.528	0.284	-0.046	0.209
TMAX	0.145	0.197	0.006	0.117	0.283	-0.043	-0.144	0.258	0.500	0.183	-0.017	0.221
TMIN	0.208	0.094	0.112	0.087	0.191	0.083	0.207	0.251	0.503	0.489	0.091	0.251

Previous year   Current year

Figure 3. The correlation coefficients between the tree-ring index and climatic factors (PRE, TAVE, TMAX, and TMIN indicate monthly precipitation, mean temperature, maximum temperature, and minimum temperature, respectively).
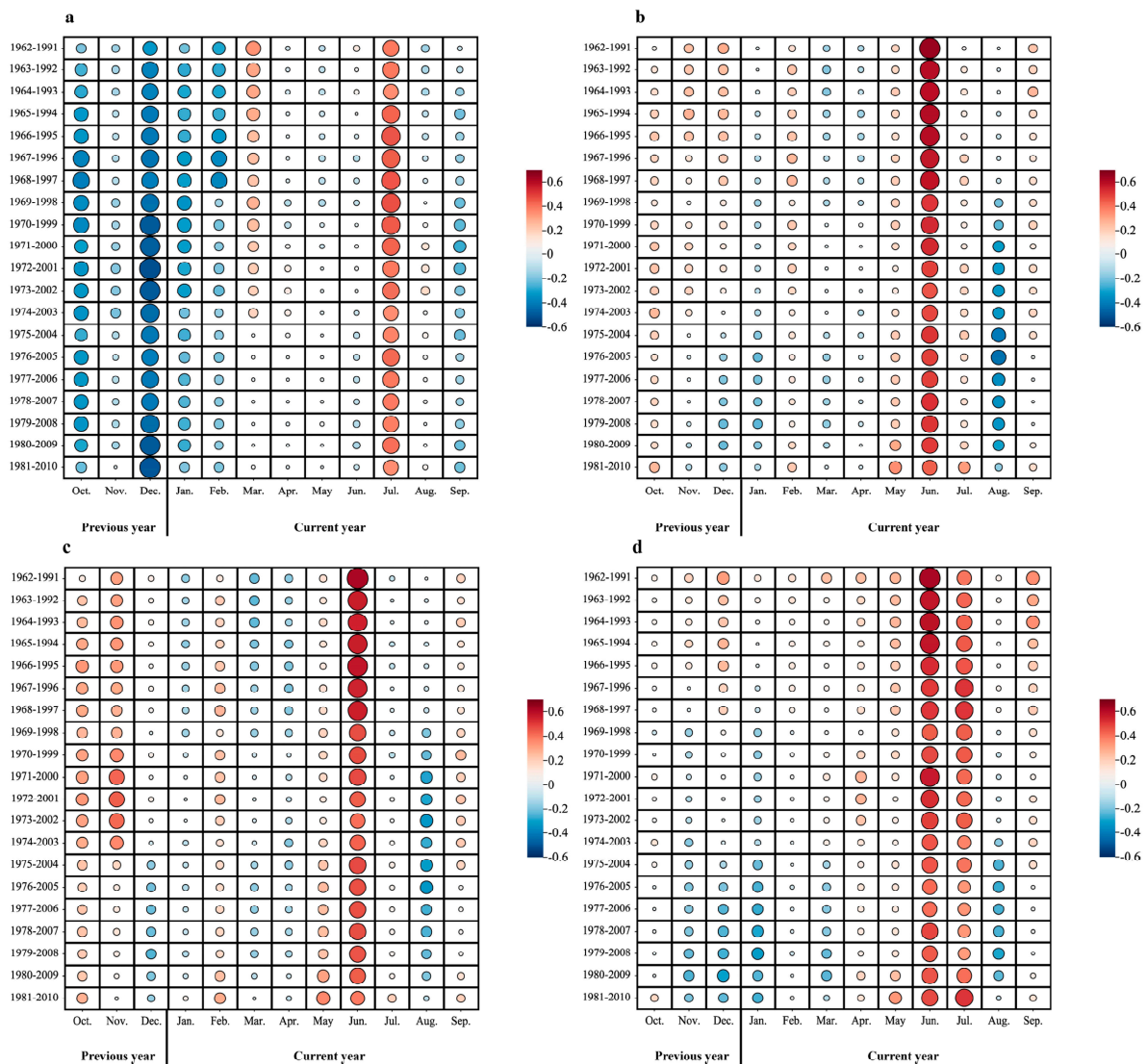

Figure 4. The 31–year moving correlations between the tree-ring index and climatic factors (**a–d**) indicate the relationship between TRW and monthly precipitation, mean temperature, maximum temperature, and minimum temperature, respectively).

3.2. Temperature Reconstruction

According to the above analysis, linear regression equation was established by taking the tree-ring index as the independent variable and the July–June average minimum temperature ($Tmin_{JJ}$) as the dependent variables:

$$T_{JJ} = 9.029 + 3.499 \times I$$

where T_{JJ} is the reconstructed June–July mean minimum temperature, and I is the growth index for the total period of calibration (1733–2010). The reconstruction equation explained 36.2% of the variance of the $Tmin_{JJ}$ series in the region, which was 34.9% after adjusting the degree of freedom, and the correlation coefficient was 0.602 (n = 49, $p < 0.001$).

The equation was tested through leave-one-out cross-validation (LOOCV), and the statistics in each test are summarized in Table 2. Here, the reduced error (RE = 0.36), mean product (t = 3.07), correlation coefficient (r = 0.602), and F-test statistic (F = 26.733) all reached a 0.01 significance level, indicating the stability of the reconstruction equation. Meanwhile, the sign tests and sign tests of the first-order difference between the reconstructed and measured values both reached a 0.01 significance level, suggesting a good reconstruction effect when using the reconstruction equation on both low-frequency and high-frequency variations. As shown in Figure 5a, the observed and reconstructed $Tmin_{JJ}$ values were very consistent in the instrumental period (1962–2010).

Table 2. Test statistics in leave-one-out cross-validation of the regression equation.

Time Period	Correlation Coefficient	Variance Explanation	F-Value	Sign Tests	Sign Tests of First-Order Difference	Mean Product (t)	Reduced Error (RE)
1962~2010	0.602	36.2%	26.733	36 (32 *, 34 **)	34 (32 *, 34 **)	3.07	0.36

Note: * and ** are the numbers of same signs needed for 0.05 and 0.01 significance levels, respectively.

3.3. Temperature Variation Characteristics

Figure 5b presents variations in the reconstructed $Tmin_{JJ}$ over 278 years (1733~2010). Here, the mean value of the reconstructed temperature series is 12.5 °C; the highest and lowest values of $Tmin_{JJ}$ are 11.0 °C (in 1798) and 13.6 °C (in 2010), respectively, with a standard deviation (SD) of 0.4 °C. Ultimately, 13 and 20 years, respectively, were found to be extremely warm and cold years over the past 278 years (Table 3), accounting for 4.3% and 7.2% of the period. Therein, 1858~1859 and 1983~1984 featured persistent extremely warm years for two or more years, while 1797~1799, 1819~1820, 1843~1844, 1874~1875, 1907~1908, and 2003~2004 featured persistent extremely cold years for two or more years.
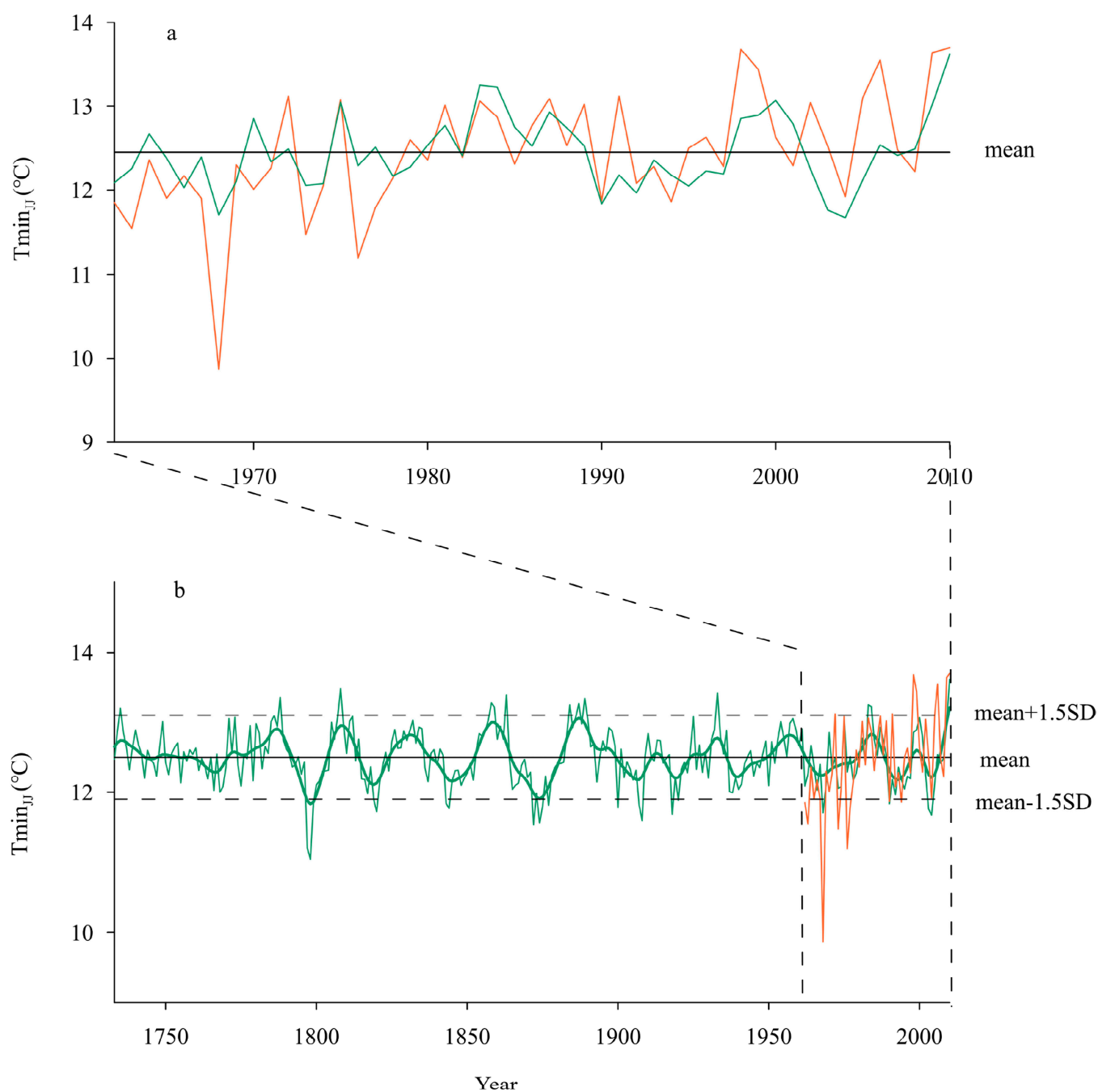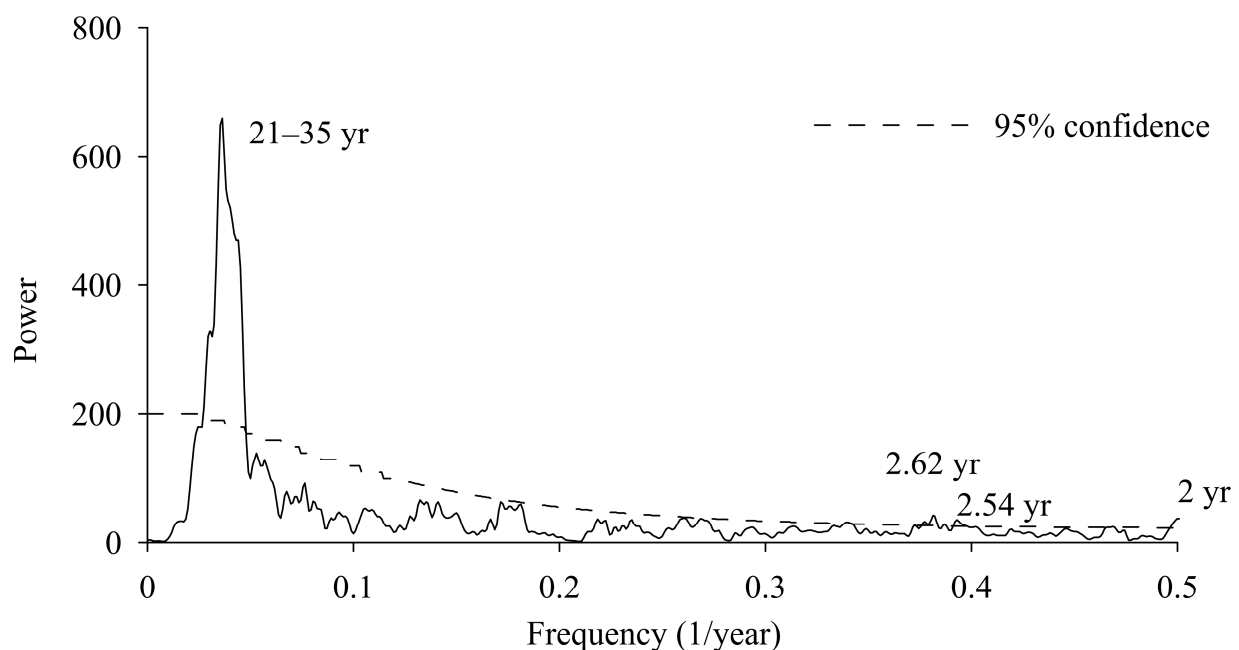
Figure 5. Comparisons between the reconstructed and observed July–June average minimum temperature (Tmin$_{JJ}$) during the period of 1962~2010 (**a**) and the reconstructed Tmin$_{JJ}$ in the reliable period of 1733~2010 (**b**). The thin orange and green lines represent the observed and reconstructed Tmin$_{JJ}$, respectively. The thick green line indicates 11-year low-pass filtering of the reconstruction.

Table 3. Extreme events during the past 278 years.

Year	The Value of Extremely High Temperature (°C)	Year	The Value of Extremely High Temperature (°C)
1735	13.2	1797	11.2
1788	13.4	1798	11.0
1808	13.5	1799	11.8
1858	13.3	1819	11.9
1859	13.2	1820	11.7
1863	13.4	1843	11.8
1884	13.2	1844	11.8
1887	13.3	1872	11.5
1889	13.3	1874	11.6
1933	13.4	1875	11.8
1983	13.2	1878	11.8
1984	13.2	1900	11.8
2010	13.6	1907	11.8
		1908	11.6
		1918	11.7
		1920	11.9
		1968	11.7
		1990	11.8
		2003	11.8
		2004	11.7

During 1733~2010, there were nine warm periods and ten cold periods. The warm periods occurred in 1733~1743, 1771~1791, 1804~1814, 1825~1837, 1853~1864, 1881~1899, 1924~1936, 1950~1962, and 1980~1988; the cold periods happened in 1759~1770, 1792~1803, 1815~1824, 1838~1852, 1865~1880, 1900~1911, 1915~1923, 1937~1949, 1963~1979, and 1989~1997.

As shown in Figure 6, the results of MTM at a confidence level of 95% indicated that the reconstructed series mainly features an interannual variation period of 2 years and a decadal oscillation period of 21 to 35 years.

Figure 6. MTM analyses for the reconstructed summer minimum temperature.

4. Discussion

4.1. Climate Responses

As shown in Figures 3 and 4, the summer temperatures (June and July), particularly the minimum temperatures, are the leading limiting factor influencing the radial growth of trees in the region. The samples were established near the alpine timberline in the central part of WSP, where the climate is mainly driven by the East Asian monsoon (EAM) and South Asian monsoon (SAM). In summer, it becomes rainy and hot, which coincides with the most vigorous and rapid growth of trees in the region. The high temperatures in summer are favorable for the photosynthesis of trees. Particularly, a higher minimum temperature can promote the accumulation of nutrients produced by photosynthesis and accelerate the splitting of cambial cells, which is conducive to the production of wide tree rings [32,33]. Conversely, a lower minimum temperature in summer not only limits the accumulation of photosynthesis products but can also affect the root system development and water uptake of trees [34,35], thus forming narrow tree rings and even frost rings or missing rings. Therefore, the mean minimum temperature in summer is the main limiting factor that affects the growth of *Abies faxoniana* and has specific physiological significance. Similar climatic limiting factors were also found in others research focusing on high-altitude or high-latitude areas [32,36–38].

In addition, correlation analysis showed that precipitation also affected the radial growth of *Abies faxoniana*, with precipitation in December of the previous year and the current July showing significant negative and positive correlations with the tree-ring index, respectively. In winter, precipitation mainly occurs in the form of snow, and more precipitation in winter may lead to a longer duration of snow cover, thus delaying cambial activity and shortening the reproductive period [39–41], resulting in a narrower tree-ring width. In contrast, greater precipitation in summer compensates for the evaporation of soil water, which facilitates root activity and photosynthesis, thus promoting the radial growth of trees.

4.2. Verification of the Reconstructed Temperature

It is necessary to explore whether the regional representativeness of the reconstructed series is consistent with the observed series across a large range. To this end, spatial correlation analysis was conducted for the reconstructed and the observed $Tmin_{JJ}$ using the grid data of the Climate Research Unit (CRU TS4.06) in the same period. The results are shown in Figure 7. Here, the spatial correlations of observed (Figure 7a) and reconstructed $Tmin_{JJ}$ (Figure 7b) values with CRU data exhibit similar spatial patterns, suggesting high representativeness of the reconstructed $Tmin_{JJ}$ for the WSP and QTP. However, due to the possibility of the loss of some variation characteristics in the reconstruction, the correlations between the reconstructed $Tmin_{JJ}$ and CRU data were weaker than those of the observed and CRU data.
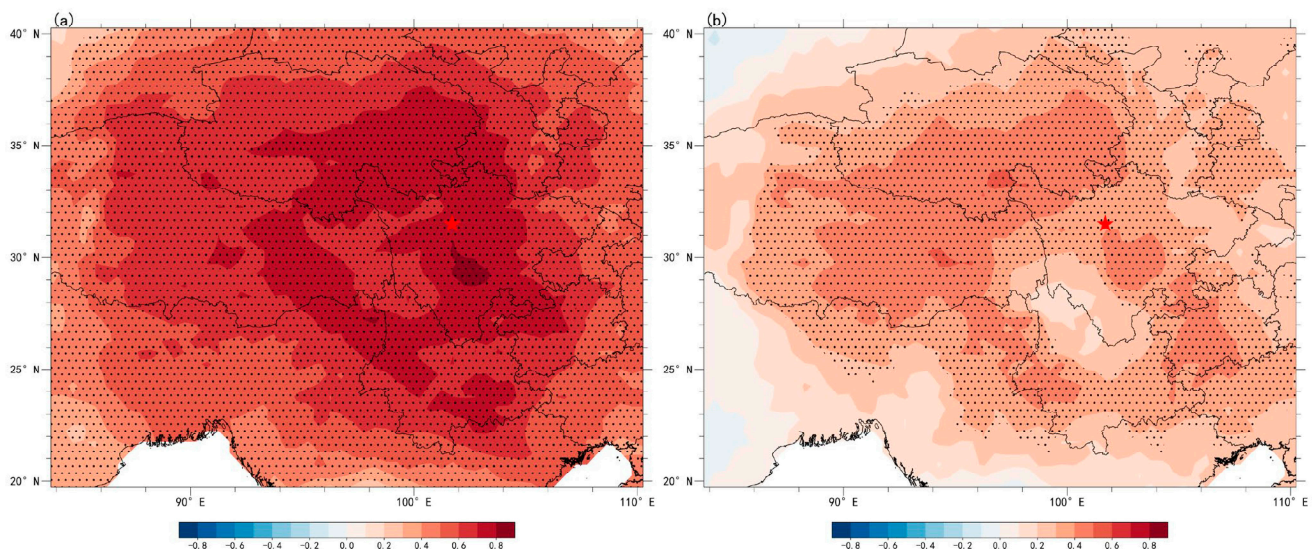
Figure 7. Spatial correlations of observed (**a**) and reconstructed (**b**) Tmin$_{JJ}$ with CRU data during the period of 1962~2010. The dotted area indicates 95% confidence.

To verify the reliability of the reconstructed series, the reconstructed series was compared with some reconstructed temperature series in surrounding areas (Figure 8). The reconstructed series for comparison and validation included the mean maximum temperature in May and June in the southeastern Qinghai–Tibet Plateau reconstructed by Zhang et al. [17], the anomaly series of mean minimum temperatures in summer in the Yangtze River headwater region reconstructed by Liang et al. [33], and the PC1 series reflecting mean minimum temperatures in the Western Sichuan Plateau reconstructed by Shao and Fan [42]. During the comparison, 11-year Gaussian low-pass filtering was performed for all series. As shown in Figure 8, despite certain differences in the reconstruction seasons and objects, the reconstructed Tmin$_{JJ}$ in the current research presented high consistency with cold and warm periods of the other three reconstructions. This result further validated the reliability of the reconstructed series. The cold and warm periods that were well reflected by all of the four reconstructions included warm periods in the 1780s, 1810s, 1830s, 1880s~1890s, 1950s, and 1980s and common cold periods in the 1790s, 1870s, and 1960s. Except for the aforementioned cold and warm periods, the warm periods in the early 1750s and 1850s and the cold periods in the 1760s and 1840s were also commonly reflected by three reconstructed series (including those in this study). In addition, the four reconstructions also differed in their views of cold and warm periods. These differences may arise from the discrepancy in local climate due to different reconstruction time periods, reconstruction objects (maximum or minimum temperatures), and habitats at different samples. These differences may occur because of the deviations caused by the use of different detrending methods when presenting the chronologies. Some other reconstructions also recorded the cold and warm periods reflected by the reconstructed Tmin$_{JJ}$ in this study. The continuous cold period from 1900~1923 was also reflected by the reconstructed temperature variations of southeastern QTP in winter [43], the mean temperatures in June and July in the WSP [18], the mean temperatures from June to August in the Eastern QTP [44], and the mean temperature field during May and June in the southeastern QTP [2]. The warm period from 1950 to 1962 was also well reflected by the reconstructed annual mean minimum temperatures in Hengduan Mountains [37] and the annual mean temperatures in Songpan [45].
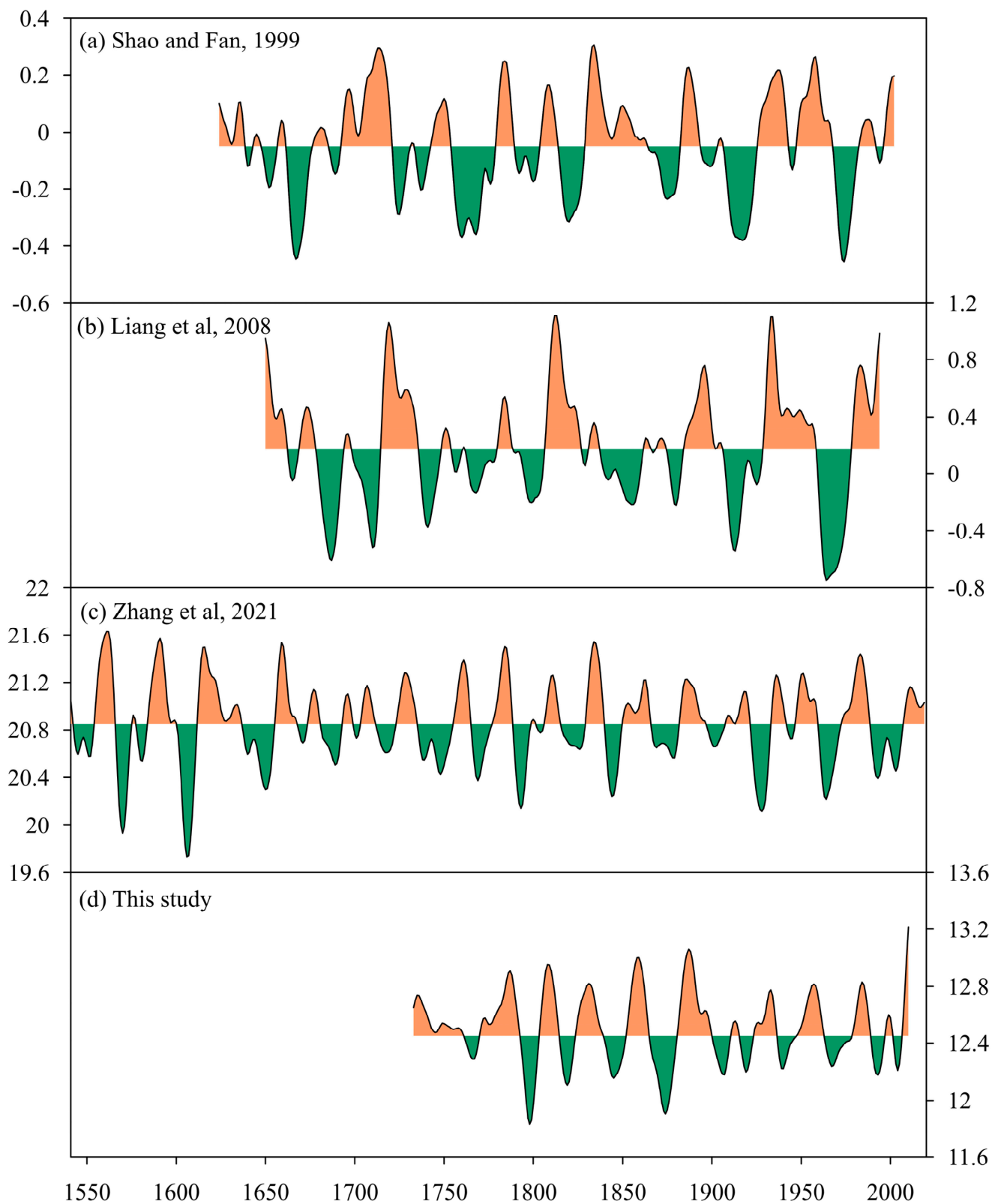
Figure 8. Comparisons between our reconstruction and other proxies: (**a**) PC1 series reflecting mean minimum temperatures in the WSP [42]; (**b**) the anomaly series of mean minimum temperatures in summer in the Yangtze River headwater region [33]; (**c**) the mean maximum temperature in May and June in the southeastern Qinghai–Tibet Plateau [17], and (**d**) the reconstructed mean summer minimum temperature of the present study. Here, 11-year Gaussian low-pass filtering was performed for all series.

Although few historical climatic events before 1950 can be determined, some clues can still be garnered from historical records to provide evidence for a reconstruction. According to some low-temperature events (snow disasters and freeze-related injuries) in the Sichuan Volume of the China Meteorological Calamity Grand Ceremony [46], there were few low-temperature events, indicating a high-temperature period. Correspondingly, low-temperature events were frequently recorded in the low-temperature period. For example, 1865~1880 was found to be a cold period in our reconstruction. Correspondingly, large-scale snow disasters happened frequently from the 1860s to early 1870s, particularly in 1871, in which snow disasters were most severe: "countless passers-by died, and most cattle and sheep froze to death" [46]. Thereafter, snow disasters occurred frequently from 1890 to 1930, and snow disasters were recorded to happen in counties and cities around the study area in 1913, 1917, and 1922 [46]. This period corresponds to the two continuous cold periods from 1900 to 1911 and 1915 to 1923 in the reconstructed series.

The glacial advance and retreat around the study area also conform to the reconstruction [47–49]. The continuous low-temperature periods reflected by the reconstructed series correspond to the stable or advanced stages of glaciers. Glacial recession or significant glacial retreat were observed when the reconstructed series showed a persistent trend toward increasing temperatures or when the temperature remained high.

4.3. Climate Responses

MTM spectral analysis of the reconstruction shows that the reconstructed series included significant periodic changes (Figure 6). Furthermore, wavelet analysis indicated the significant presence of decadal oscillations with a period of 21~35 y, nearly throughout the period analyzed. The interannual periodic changes of 2 y mainly correspond to high-frequency oscillations of the reconstructed series. On the one hand, this result is likely related to the quasi-two-year period commonly present in the climatic system; on the other hand, these changes are consistent with the main period of El Niño–Southern Oscillation (ENSO), indicating that ENSO may have a certain modulating effect on temperature variations in the region. Similar results were also obtained for the reconstructed temperature in the surrounding areas [17,21,50,51]. The decadal periodic oscillation is likely related to Pacific decadal oscillation (PDO), which was verified in numerous studies as one of the main factors controlling decadal climate variability in East Asia [17,52,53]. The reconstructed series has a correlation coefficient of 0.14 with the reconstructed PDO [54] (1733~2004, $p < 0.05$), indicating that PDO exerts an important influence on the temperature in the study area. Here, when PDO is in a warm phase, the sea temperature in the middle-east equator of the Pacific Ocean is higher, and the location of the ridge point of the western Pacific subtropical high (WPSH) is much more westward. The study area is likely to be controlled by WPSH, with strong downdrafts leading to higher temperatures. Conversely, if PDO is in a cold phase, it becomes conducive to the northward movement of warm and humid air flows, leading to frequent rain and relatively lower summer temperatures in the study area. Studies in the nearby area revealed that PDO is one of the main controlling factors [55,56]. Correlations between the reconstructed series and sea surface temperature (SST) of the Pacific also support this result (Figure 9).
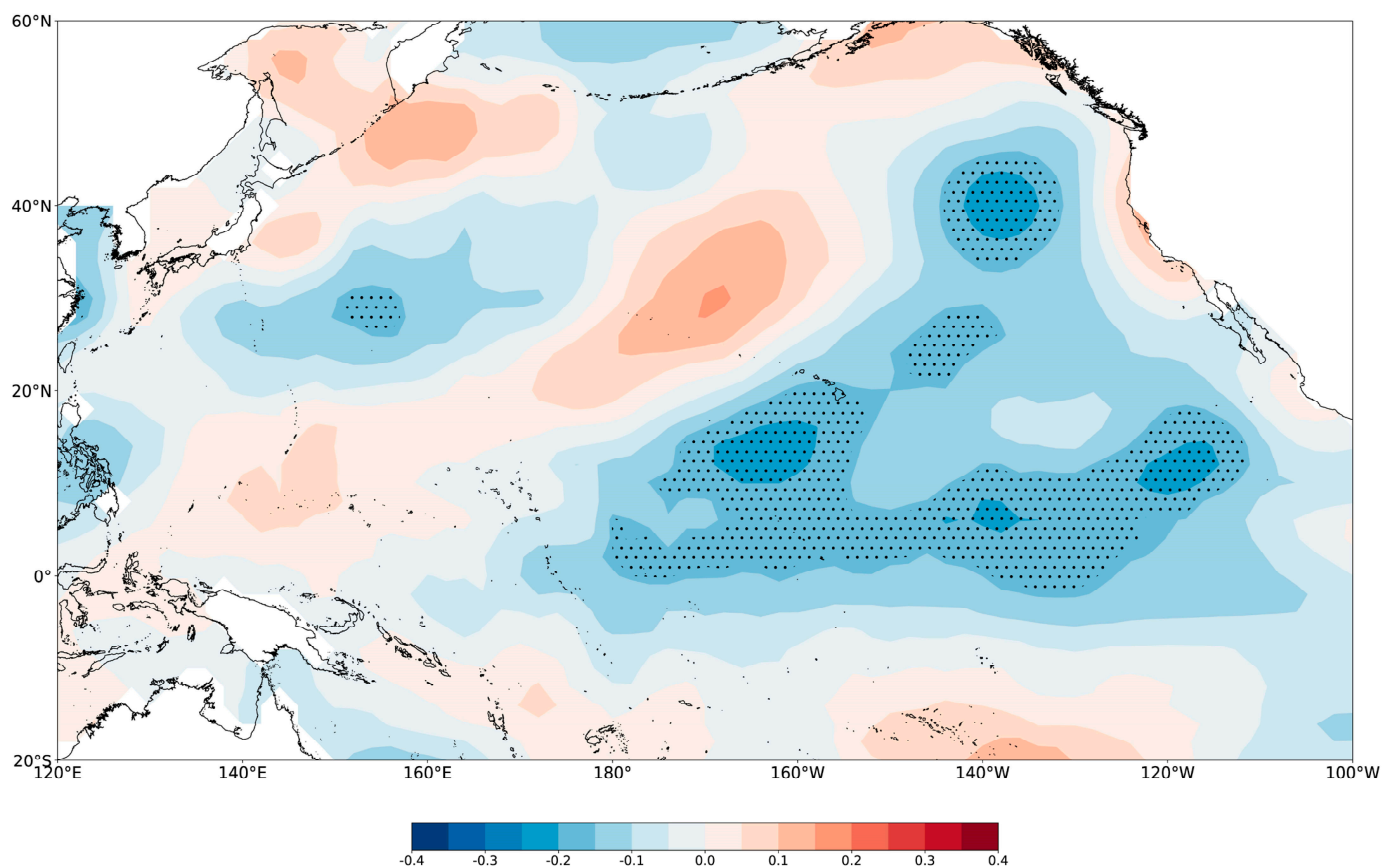
Figure 9. Spatial correlations between the reconstruction and sea surface temperature (SST) during the period of 1854–2010. The dotted area indicates 95% confidence.

5. Conclusions

TRW chronologies were constructed using tree-ring samples of *Abies faxoniana* collected on the Snowy Mountains in Dadu River Basin in the central part of WSP. The summer (June and July) mean minimum temperature was reconstructed for the period of 1733~2010. The reconstruction equation was found to be stable and reliable, with a variance explanation rate of 36.2% in the observed period (1962~2010). A total of 13 years of extremely high temperatures and 20 years of extremely low temperatures occurred in the past 278 years. In addition, there were 9 warm periods and 10 cold periods on a decadal scale. The correlation analysis shows that the reconstruction is highly spatiotemporally representative. Moreover, the reconstruction could be verified by other temperatures reconstructed using tree-ring data, historical meteorological disaster records, and glacial advance and retreat events in surrounding areas. The MTM results suggest that there were significant quasi-2-year and 21–35-year cycles in temperature variation in the study area. ENSO and PDO were possibly important controlling factors of temperature variations in the region. The reconstruction results indicate greater historical climate change at the western Sichuan Plateau and provide a reference for tackling climate change.

Author Contributions: Conceptualization, J.L. and L.J.; methodology, J.L.; software, J.L.; validation, J.L. and Z.Z.; formal analysis, J.L.; investigation, J.L. and Z.Z.; resources, L.J.; data curation, Z.Z.; writing—original draft preparation, J.L.; writing—review and editing, L.J. and J.L.; visualization, J.L.; supervision, L.J.; project administration, J.L. and L.J.; funding acquisition, J.L. and L.J. All authors have read and agreed to the published version of the manuscript.

References

1. Deng, Y.; Gou, X.; Gao, L.; Yang, M.; Zhang, F. Spatiotemporal Drought Variability of the Eastern Tibetan Plateau during the Last Millennium. *Clim. Dyn.* **2017**, *49*, 2077–2091. [CrossRef]
2. Li, J.; Jin, L.; Zheng, Z.; Qin, N. Variability of the Early Summer Temperature in the Southeastern Tibetan Plateau in Recent Centuries and the Linkage to the Indian Ocean Basin Mode. *Lithosphere* **2022**, *2022*, 9648384. [CrossRef]
3. Gou, X.; Deng, Y.; Chen, F.; Yang, M.; Fang, K.; Gao, L.; Yang, T.; Zhang, F. Tree Ring Based Streamflow Reconstruction for the Upper Yellow River over the Past 1234 Years. *Chin. Sci. Bull.* **2010**, *55*, 4179–4186. [CrossRef]
4. Li, J.; Xie, S.-P.; Cook, E.R.; Chen, F.; Shi, J.; Zhang, D.D.; Fang, K.; Gou, X.; Li, T.; Peng, J.; et al. Deciphering Human Contributions to Yellow River Flow Reductions and Downstream Drying Using Centuries-Long Tree Ring Records. *Geophys. Res. Lett.* **2019**, *46*, 898–905. [CrossRef]
5. Shi, F.; Sun, C.; Guion, A.; Yin, Q.; Zhao, S.; Liu, T.; Guo, Z. Roman Warm Period and Late Antique Little Ice Age in an Earth System Model Large Ensemble. *J. Geophys. Res. Atmos.* **2022**, *127*, e2021JD035832. [CrossRef]
6. Jiang, D.; Yu, G.; Zhao, P.; Chen, X.; Liu, J.; Liu, X.; Wang, S.; Zhang, Z.; Yu, Y.; Li, Y.; et al. Paleoclimate Modeling in China: A Review. *Adv. Atmos. Sci.* **2015**, *32*, 250–275. [CrossRef]
7. Parsons, L.A.; Amrhein, D.E.; Sanchez, S.C.; Tardif, R.; Brennan, M.K.; Hakim, G.J. Do Multi-Model Ensembles Improve Reconstruction Skill in Paleoclimate Data Assimilation? *Earth Space Sci.* **2021**, *8*, e2020EA001467. [CrossRef]
8. Pang, H.; Hou, S.; Zhang, W.; Wu, S.; Jenk, T.M.; Schwikowski, M.; Jouzel, J. Temperature Trends in the Northwestern Tibetan Plateau Constrained by Ice Core Water Isotopes Over the Past 7000 Years. *J. Geophys. Res. Atmos.* **2020**, *125*, e2020JD032560. [CrossRef]
9. Gyawali, A.R.; Wang, J.; Ma, Q.; Wang, Y.; Xu, T.; Guo, Y.; Zhu, L. Paleo-Environmental Change since the Late Glacial Inferred from Lacustrine Sediment in Selin Co, Central Tibet. *Palaeogeogr. Palaeoclimatol. Palaeoecol.* **2019**, *516*, 101–112. [CrossRef]
10. Chinese Academy of Meteorological Sciences; China Meteorological Administration. *Yearly Charts of Dryness/Wetness in China for the Last 500-Year Period*; SinoMaps Press: Beijing, China, 1981.
11. Yang, B.; Qin, C.; Bräuning, A.; Osborn, T.J.; Trouet, V.; Ljungqvist, F.C.; Esper, J.; Schneider, L.; Grießinger, J.; Büntgen, U.; et al. Long-Term Decrease in Asian Monsoon Rainfall and Abrupt Climate Change Events over the Past 6700 Years. *Proc. Natl. Acad. Sci. USA* **2021**, *118*, e2102007118. [CrossRef]
12. Liu, Y.; Song, H.; An, Z.; Sun, C.; Trouet, V.; Cai, Q.; Liu, R.; Leavitt, S.W.; Song, Y.; Li, Q.; et al. Recent Anthropogenic Curtailing of Yellow River Runoff and Sediment Load Is Unprecedented over the Past 500 y. *Proc. Natl. Acad. Sci. USA* **2020**, *117*, 18251–18257. [CrossRef]
13. PAGES 2k. Consortium Continental-Scale Temperature Variability during the Past Two Millennia. *Nat. Geosci.* **2013**, *6*, 339–346. [CrossRef]
14. Neukom, R.; Steiger, N.; Gómez-Navarro, J.J.; Wang, J.; Werner, J.P. No Evidence for Globally Coherent Warm and Cold Periods over the Preindustrial Common Era. *Nature* **2019**, *571*, 550–554. [CrossRef]
15. Mann, M.E.; Bradley, R.S.; Hughes, M.K. Global-Scale Temperature Patterns and Climate Forcing over the Past Six Centuries. *Nature* **1998**, *392*, 779–787. [CrossRef]
16. Li, H.; Liu, L.; Shan, B.; Xu, Z.; Niu, Q.; Cheng, L.; Liu, X.; Xu, Z. Spatiotemporal Variation of Drought and Associated Multi-Scale Response to Climate Change over the Yarlung Zangbo River Basin of Qinghai–Tibet Plateau, China. *Remote Sens.* **2019**, *11*, 1596. [CrossRef]
17. Zhang, Y.; Li, J.; Zheng, Z.; Zeng, S. A 479-Year Early Summer Temperature Reconstruction Based on Tree-Ring in the Southeastern Tibetan Plateau, China. *Atmosphere* **2021**, *12*, 1251. [CrossRef]
18. Zhang, Y.; Li, J.; Wang, S.; Shao, X.; Qin, N.; An, W. A Reconstruction of June–July Temperature since AD 1383 for Western Sichuan Plateau, China Using Tree-Ring Width. *Int. J. Climatol.* **2022**, *42*, 1803–1817. [CrossRef]
19. Li, J.; Li, J.; Li, T.; Au, T.F. 351-Year Tree Ring Reconstruction of the Gongga Mountains Winter Minimum Temperature and Its Relationship with the Atlantic Multidecadal Oscillation. *Clim. Change* **2021**, *165*, 49. [CrossRef]
20. Fang, K.; Guo, Z.; Chen, D.; Wang, L.; Dong, Z.; Zhou, F.; Zhao, Y.; Li, J.; Li, Y.; Cao, X. Interdecadal Modulation of the Atlantic Multi-Decadal Oscillation (AMO) on Southwest China's Temperature over the Past 250 Years. *Clim. Dyn.* **2019**, *52*, 2055–2065. [CrossRef]
21. Nie, W.; Li, M. July Mean Temperature Reconstruction for the Southern Tibetan Plateau Based on Tree-Ring Width Data during 1763–2020. *Forests* **2022**, *13*, 1911. [CrossRef]
22. Zhu, L.; Zhang, Y.; Li, Z.; Guo, B.; Wang, X. A 368-Year Maximum Temperature Reconstruction Based on Tree-Ring Data in the Northwestern Sichuan Plateau (NWSP), China. *Clim. Past* **2016**, *12*, 1485–1498. [CrossRef]

23. Xu, G.; Liu, X.; Zhang, Q.; Zhang, Q.; Hudson, A.; Trouet, V. Century-Scale Temperature Variability and Onset of Industrial-Era Warming in the Eastern Tibetan Plateau. *Clim Dyn* **2019**, *53*, 4569–4590. [CrossRef]
24. Fritts, H. *Tree Rings and Climate*; Elsevier: Amsterdam, The Netherlands, 2012.
25. Fritts, H.C. Dendroclimatology and Dendroecology. *Quat. Res.* **1971**, *1*, 419–449. [CrossRef]
26. Holmes, R.L. Computer-Assisted Quality Control in Tree-Ring Dating and Measurement. *Tree-Ring Bull.* **1983**, *43*, 51–67.
27. Cook, E.R. A Time Series Analysis Approach to Tree Ring Standardization. Ph.D. Thesis, University of Arizona, Tuscon, AZ, USA, 1985.
28. Wigley, T.M.L.; Briffa, K.R.; Jones, P.D. On the Average Value of Correlated Time Series, with Applications in Dendroclimatology and Hydrometeorology. *J. Appl. Meteorol. Climatol.* **1984**, *23*, 201–213. [CrossRef]
29. An, W.; Li, J.; Wang, S.; Xu, C.; Shao, X.; Qin, N.; Guo, Z. Hydrological Extremes in the Upper Yangtze River over the Past 700 Yr Inferred from a Tree Ring Δ18O Record. *J. Geophys. Res. Atmos.* **2022**, *127*, e2021JD036109. [CrossRef]
30. Babadi, B.; Brown, E.N. A Review of Multitaper Spectral Analysis. *IEEE Trans. Biomed. Eng.* **2014**, *61*, 1555–1564. [CrossRef]
31. Prieto, G.A.; Parker, R.L.; Vernon, F.L., III. A Fortran 90 Library for Multitaper Spectrum Analysis. *Comput. Geosci.* **2009**, *35*, 1701–1710. [CrossRef]
32. Huang, R.; Zhu, H.; Liang, E.; Asad, F.; Grießinger, J. A Tree-Ring–Based Summer (June–July) Minimum Temperature Reconstruction for the Western Kunlun Mountains since AD 1681. *Theor. Appl. Climatol.* **2019**, *138*, 673–682. [CrossRef]
33. Liang, E.; Shao, X.; Qin, N. Tree-Ring Based Summer Temperature Reconstruction for the Source Region of the Yangtze River on the Tibetan Plateau. *Glob. Planet. Change* **2008**, *61*, 313–320. [CrossRef]
34. Mayr, S. Limits in Water Relations. In *Trees at Their Upper Limit: Treelife Limitation at the Alpine Timberline*; Springer: Berlin/Heidelberg, Germany, 2007; pp. 145–162.
35. Wieser, G.; Tausz, M. *Trees at Their Upper Limit: Treelife Limitation at the Alpine Timberline*; Springer Science & Business Media: Berlin/Heidelberg, Germany, 2007; Volume 5.
36. Shi, C.; Wang, K.; Sun, C.; Zhang, Y.; He, Y.; Wu, X.; Gao, C.; Wu, G.; Shu, L. Significantly Lower Summer Minimum Temperature Warming Trend on the Southern Tibetan Plateau than over the Eurasian Continent since the Industrial Revolution. *Environ. Res. Lett.* **2019**, *14*, 124033. [CrossRef]
37. Keyimu, M.; Li, Z.; Zhang, G.; Fan, Z.; Wang, X.; Fu, B. Tree Ring–Based Minimum Temperature Reconstruction in the Central Hengduan Mountains, China. *Theor. Appl. Climatol.* **2020**, *141*, 359–370. [CrossRef]
38. Liang, E.; Wang, Y.; Piao, S.; Lu, X.; Camarero, J.J.; Zhu, H.; Zhu, L.; Ellison, A.M.; Ciais, P.; Peñuelas, J. Species Interactions Slow Warming-Induced Upward Shifts of Treelines on the Tibetan Plateau. *Proc. Natl. Acad. Sci. USA* **2016**, *113*, 4380–4385. [CrossRef]
39. Vaganov, E.A.; Hughes, M.K.; Kirdyanov, A.V.; Schweingruber, F.H.; Silkin, P.P. Influence of Snowfall and Melt Timing on Tree Growth in Subarctic Eurasia. *Nature* **1999**, *400*, 149–151. [CrossRef]
40. D'Arrigo, R.; Wilson, R.; Liepert, B.; Cherubini, P. On the 'Divergence Problem' in Northern Forests: A Review of the Tree-Ring Evidence and Possible Causes. *Glob. Planet. Change* **2008**, *60*, 289–305. [CrossRef]
41. Linderholm, H.W.; Chen, D. Central Scandinavian Winter Precipitation Variability during the Past Five Centuries Reconstructed from Pinus Sylvestris Tree Rings. *Boreas* **2008**, *34*, 43–52. [CrossRef]
42. Shao, X.; Fan, J. Past Climate on West Sichuan Plateau as Reconstructed from Ring-Widths of Dragon Spruce. *Quat. Sci.* **1999**, *1*, 81–89.
43. Huang, R.; Zhu, H.; Liang, E.; Liu, B.; Shi, J.; Zhang, R.; Yuan, Y.; Grießinger, J. A Tree Ring-Based Winter Temperature Reconstruction for the Southeastern Tibetan Plateau since 1340 CE. *Clim. Dyn.* **2019**, *53*, 3221–3233. [CrossRef]
44. Wang, J.; Yang, B.; Ljungqvist, F.C. A Millennial Summer Temperature Reconstruction for the Eastern Tibetan Plateau from Tree-Ring Width. *J. Clim.* **2015**, *28*, 5289–5304. [CrossRef]
45. Li, J.; Shao, X.; Li, Y.; Qin, N. Annual Temperature Recorded in Tree-Ring from Songpan Region. *Chin. Sci. Bull.* **2014**, *59*, 1446–1458.
46. Wen, K.; Zhan, Z. *China Meteorological Calamity Grand Ceremony: Sichuan*; Meteorological Press: Beijing, China, 2005.
47. Xu, X.; Yi, C. Little Ice Age on the Tibetan Plateau and Its Bordering Mountains: Evidence from Moraine Chronologies. *Glob. Planet. Change* **2014**, *116*, 41–53. [CrossRef]
48. Xu, P.; Zhu, H.; Shao, X.; Yin, Z. Tree Ring-Dated Fluctuation History of Midui Glacier since the Little Ice Age in the Southeastern Tibetan Plateau. *Sci. China Earth Sci.* **2012**, *55*, 521–529. [CrossRef]
49. Li, Z.; He, Y.; Jia, W. Response of"Glaciers-Runoff"System in a Typical Temperate-Glacier, Hailuogou Glacier in Gongga Mountain of China to Global Change. *Sci. Geogr. Sin.* **2008**, *28*, 229.
50. Liu, N.; Bao, G.; Liu, Y.; Linderholm, H.W. Two Centuries-Long Streamflow Reconstruction Inferred from Tree Rings for the Middle Reaches of the Weihe River in Central China. *Forests* **2019**, *10*, 208. [CrossRef]
51. Su, M.; Wang, H. Relationship and Its Instability of ENSO—Chinese Variations in Droughts and Wet Spells. *Sci. China Ser. D* **2007**, *50*, 145–152. [CrossRef]
52. Yin, H.; Liu, H.; Linderholm, H.W.; Sun, Y. Tree Ring Density-Based Warm-Season Temperature Reconstruction since a.D. 1610 in the Eastern Tibetan Plateau. *Palaeogeogr. Palaeoclimatol. Palaeoecol.* **2015**, *426*, 112–120. [CrossRef]
53. Yin, H.; Li, M.-Y.; Huang, L. Summer Mean Temperature Reconstruction Based on Tree-Ring Density over the Past 440 Years on the Eastern Tibetan Plateau. *Quat. Int.* **2021**, *571*, 81–88. [CrossRef]

54. D'Arrigo, R.; Wilson, R. Spring Pacific Decadal Oscillation Index Reconstruction. In *IGBP PAGES/World Data Center for Paleoclimatology Data Contribution Series*; World Data Center for Paleoclimatology: Boulder, CO, USA, 2006; Volume 95.

55. Qin, J.; Tian, Y.; Ren, J.; Wan, Y. Interdecadal Oscillation of Pacific and Interdecadal Change of Summer Temperature in Yunnan. *Plateau Meteor* **2004**, *23*, 69–76.

56. Yang, Y.; Zhao, D.; Chen, H. Variability of Bio-Climatology Indicators in the Southwest China under Climate Warming during 1961–2015. *Int. J. Biometeorol.* **2019**, *63*, 107–119. [CrossRef]